Residual CTAB Ligands as Mass Spectrometry Labels to Monitor Cellular Uptake of Au Nanorods

Isabel García,[a,b] Malou Henriksen-Lacey,[a] Ana Sánchez-Iglesias,[a] Marek Grzelczak,[a,c] Soledad Penadés,[a,b,] Luis M. Liz-Marzán[a,b,c,]**

[a]*CIC biomaGUNE, Paseo de Miramón 182, 20009 Donostia-San Sebastián, Spain.*

[b]*Biomedical Research Networking Center in Bioengineering, Biomaterials, and Nanomedicine (CIBER-BBN), PaseoMiramón 182 , 20009 Donostia- San Sebastián, Spain.*

[c]*Ikerbasque, Basque Foundation for Science, 48013 Bilbao, Spain*

*Corresponding authors' e-mail:

spenades@cicbiomagune.es (S. Penadés); llizmarzan@cicbiomagune.es (L.M. Liz-Marzán)

ABSTRACT:

Gold nanorods have numerous applications in biomedical research, including diagnostics, bioimaging and photothermal therapy. Even though surfactant removal and surface conjugation with anti-fouling molecules such as polyethylene glycol (PEG) are required to minimize non-specific protein binding and cell uptake, the reliable characterization of these processes remains challenging. We propose here the use of laser desorption/ionization mass spectrometry (LDI-MS) to study the efficiency of ligand exchange of cetyltrimethylammonium bromide (CTAB)-coated nanorods with different PEG grafting densities and to characterize nanorod internalization in cells. Application of LDI-MS analysis shows that residual CTAB consistently remains adsorbed on PEG-capped Au nanorods. Interestingly, such residual CTAB can be exploited as a mass barcode to discern the presence of nanorods in complex fluids and *in vitro* cellular systems, even at very low concentrations.

TOC GRAPHICS

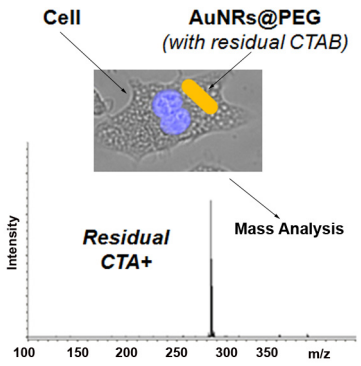

Gold nanorods (AuNRs) have been widely adopted for biological applications due to their unique plasmonic properties. As light interacts with AuNRs, localized surface plasmon resonances (LSPR) are excited, leading to strong absorption and scattering of light in the visible-near IR (NIR) range[1] and in turn rendering AuNRs promising candidates for bioimaging and biosensing.[2,3] Such biological applications require detailed understanding of how the nanoparticle surface chemistry can influence interactions with proteins and cells. The most convenient and widespread synthesis method to prepare AuNRs is known as seed-mediated growth.[4]This chemical method has been largely optimized to yield quasi-monodisperse AuNRs with narrow LSPR resonances in the visible and NIR. The synthesis typically involves the use of the surfactant cetyltrimethylammonium bromide (CTAB) as a morphology directing agent, but also as a stabilizer, through the formation of bilayers on the AuNR surface.[55] Unfortunately CTAB-capped AuNRs display poor stability in biological media as well as significant surfactant-driven cytotoxicity.[6,7,8,9] Several surface coatings have been proposed,[10,11,12] polyethyleneglycol (PEG) being the most usual one, to enhance biocompatibility, colloidal stability of AuNRs in physiological conditions and enable long circulation of the particles in blood due to its biofouling activity. Functionalization strategies for CTAB-coated AuNRs comprise ligand exchange of the native surfactant[13] or deposition of a passivating surfactant layer,[14,15] and usually assume that CTAB molecules cannot be easily replaced by other biomolecules/ligands from the surface of gold nanorods, but remaining molecules have been reported not to be toxic.[16] Whereas surface functionalization plays a crucial role on the properties and biological activity of nanoparticles,[17] analytical methods are not sufficiently advanced to characterize the interactions of particles with proteins or to identify adsorbed molecules that are present at a low grafting density on nanoparticlesurfaces. Gold nanoparticles offer however a unique platform for use as a matrix in

laser desorption/ionization mass spectrometry (LDI-MS), since they enable sensitive detection of biomolecules[18,19] and can serve as affinity probes for the enrichment of analytes prior to LDI-MS.[20,21] AuNRs in particular efficiently allow desorption and ionization of attached ligands from their surface, mainly due to the strong absorption of the laser energy, thereby leading to high sensitivity.[22]

The focus of this letter is a mass spectrometry analysis of AuNRs that demonstrates the presence of CTAB after ligand exchange with thiolated PEG (SH-PEG), as well as how such residual surfactant can be used as an intrinsic marker to identify the presence of nanorods, both in simple and in complex fluids, including *in vitro* cell cultures. We aimed at studying the replacement of CTAB from AuNRs with SH-PEGin different extents, and identifying the grafting densities that minimize non-specific adsorption of proteins (protein corona formation) in biological environments, by means of agarose gel electrophoresis (AGE) assays.[23,24] It has been described that the protein corona can block targeting ligands at nanoparticle surfaces,[25,26] so engineered surfaces that avoid this phenomenon have become indispensable. Quaternary ammonium ions have a strong capacity to be ionized and are well known mass spectrometry suppressors.[27] In addition, the desorption/ionization process of CTAB ligands on gold surfaces produces an enhancement in signals from CTA^+ ions with lower energy (little or no fragmentation) and the absence of Au_n^+ gold cluster ions due to the direct contact of CTAB ligands with the gold surface. We use these properties to evaluate and characterize residual CTAB molecules on the surface of AuNRs by LDI-MS as a rapid, sensitive and low sample volume technique. In addition, we also aim at monitoring the cellular uptake of AuNRs by evaluating the residual CTAB by LDI-MS. Whereas other techniques such as transmission electron microscopy (TEM), dark field optical microscopy (DFM) or surface-enhanced Raman scattering (SERS), allow

visualization of AuNPs in the cellular environment by taking advantage of the properties of the Au cores,[28,29,30] LDI-MS provides a quantitative method to determine intracellular AuNPs via the detection of adsorbed CTAB molecules. A related bulk technique that has been widely used for the evaluation of nanomaterial concentration inside cells is inductively coupled plasma mass spectrometry (ICP-MS), but digestion of the cellular matrix and NPs is required, thereby introducing variability into the measurements. LDI-MS has also been previously employed to study the stability of quantum dots in cells[31] and to assess cellular uptake of gold nanoparticles.[32] Rotello and co-workers demonstrated that the cellular uptake of small spherical Au NPs (2 nm diameter) entirely functionalized with cationic alkanethiol ligands can be monitored by MS. The authors showed that different mass barcodes were required to detect differently tagged Nps with distinct ionizable surface functionalities and the LDI mass spectra showed peaks for the molecular ions together with Au cluster fragmentations. We propose here application of this methodology to nanorods, but using residual CTAB only as a universal mass barcode signaling the presence of nanorods inside complex biological media and/or cells. It should be noted that these techniques are often complementary to fluorescence microscopy, which can also be used to determine nanoparticle uptake in living cells, but dye conjugation to the targeted nanoparticles is required and quenching effects by gold cores may occur and should be minimized.[33] We thus demonstrate here that residual CTAB molecules associated with PEG-functionalized AuNRs can be accurately detected by LDI-MS and that this can be exploited for indirect identification of the presence of AuNRs in cellular systems where complex proteins are also present, as schematically shown in **Figure 1**.

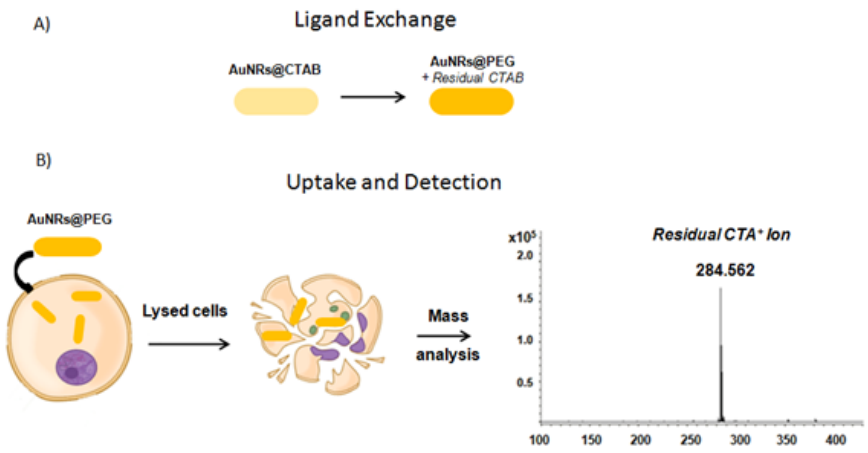

Figure 1. A) Partial replacement of CTAB from AuNRs upon ligand exchange with thiolated PEG (PEG-SH). B) Schematic representation illustrating the use of residual CTAB on PEGylated AuNRs to characterize cellular uptake by means of LDI-MS. Macrophages incubated with AuNRs@PEG are lysed, spotted onto a mass plate and AuNRs are analyzed by LDI-MS.

We prepared AuNRs with identical core sizes (38 nm x 11 nm, **Figure S1**, Supporting Information) and two different densities of PEG-SH (PEG:AuNR ratios) and residual CTAB, which we refer to as AuNRs@PEG_{Low} and AuNRs@PEG_{High}, for low and high PEG content, respectively. Recent studies revealed that surface ligand density can strongly affect the properties of nanoparticles, including resistance to protein adsorption, toxicity and cellular uptake.[34] PEGylation is highly sensitive to grafting density[35] and remaining CTAB molecules might critically influence protein binding.[36] PEG-coated spherical AuNPs with an average diameter of 14 nm (Au_{14}@PEG) were also prepared as a control for CTAB-free particles.

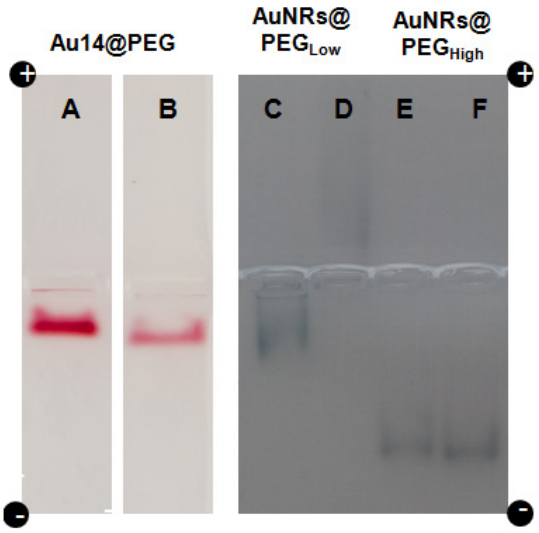

Figure 2. Results of agarose gel electrophoresis forAu_{14}@PEG, AuNRs@PEG_{Low} and AuNRs@PEG_{High} before (lines A, C, E) and after (lines B, D, F)incubation with 10%FBS, showing a shift in electrophoretic mobility for FBS incubated AuNRs@PEG_{Low} but no change for AuNRs@PEG_{High} (Line F). The band in line D is positive to Bradford staining (**Figure S2**).

To evaluate protein adsorption and PEG/CTAB grafting density, we used agarose gel electrophoresis (AGE) as a non-destructive, highly sensitive and minimal sample consuming analytical technique (**Figure 2**). AuNRs@PEG_{Low} and AuNRs@PEG_{High} were thus incubated in FBS medium (10%) and the level of protein adsorption was estimated by AGE. Before and after protein incubation, equal concentrations of Au_{14}@PEG, AuNRs@PEG_{Low} and AuNRs@PEG_{High} were loaded into an agarose gel anda voltage of 80 V was applied for 4 hours, which should allow the detection of changes in both the size and surface charge of the particles. AuNRs@PEG_{Low} and control spherical Au_{14}@PEG samples both showed a similar band prior to protein treatment, which is indicative of similar particle size and charge (**Figure 2**, columns A, C). Upon FBS treatment, a shift was observed in the electrophoretic mobility assay for AuNRs@PEG_{Low} (**Figure 2**, column D), indicating that protein adsorption induced changes in

the size and the charge of the particles. Interestingly, protein induced mobility changes did not occur for either AuNRs@PEG_{High} (**Figure 2**, column F)or Au_{14}NPs (**Figure 2**, column B), suggesting that CTAB favors protein adsorption. The main protein component in the medium was bovine serum albumin, which has an isoelectric point of 4.6, meaning that at pH 8 it has a negative surface charge (zeta potential ca. -20 mV).[37] To confirm the presence of a protein corona around AuNRs@PEG_{Low}, Bradford staining was applied to these samples (**Figure S2**, SI). A clear mobility shift and blue staining was seen for AuNRs@PEG_{Low} when incubated FBS (either at 1% or 10%). The gel-assay results were complemented by zeta potential measurements (**Table S1**, Supporting Information). It should be stressed that all PEGylated nanoparticles (Au_{14}@PEG, AuNRs@PEG_{Low} and AuNRs@PEG_{High}) were found to diffuse toward the negative electrode prior to protein treatment, even though they display slightly negative zeta potential values. AuNRs@PEG_{Low} and AuNRs@PEG_{High} (before FBS incubation) present a significantly different mobility in the gel (**Figure 2**, column D, F), while similar zeta potential values were obtained (**Table S1**). Our results are in agreement with previous work[38] reporting that the electrophoretic mobility of PEGylated AuNPs in agarose gels is a balance between frictional and electrophoretic forces. Increase of the PEG:AuNRs ratio is expected to lead to a transition from a loosely organized PEG brush to a more rigid one, thereby decreasing frictional and steric interactions with agarose, and increasing the mobility of AuNRs@PEG_{High} as compared to AuNRs@PEG_{Low} (**Figure 2**, column D *vs.* F).We additionally note that AuNRs@PEG_{Low} showed a large drop in zeta potential value upon exposure to FBS (from -5.5 to -20.9 mV), whilst such a strong change was not observed for Au_{14}@PEG and AuNRs@PEG_{High} (**Table S1**). Based on these results we conclude that AuNRs@PEG_{Low} adsorb much higher levels of FBS proteins than their AuNRs@PEG_{High} counterparts.

Whereas the above data indirectly reveal different degrees of ligand exchange between CTAB and PEG, they do not provide conclusive data regarding ligand composition (only effects of ligand composition are seen). Therefore, additional characterization of the surface chemistry was carried out by ^{1}H NMR spectroscopy and representative data are shown in **Figure 3A**. The ^{1}H-NMR spectra of both PEGylated AuNR samples display a peak at 3.62 ppm that can be clearly assigned to the PEG ligand. We tentatively assigned other peaks with significantly lower intensities to the presence of residual CTAB molecules, which undergo a chemical shift upon interaction with the gold surface. Unfortunately, the low signals of the protons from grafted CTAB as compared to the high signal of protons from PEG (most likely a saturated signal) only allow an imprecise integration which therefore cannot be used to estimate the relative grafting density between both AuNR samples. Therefore, additional characterization was performed by means of LDI-MS analysis. For both AuNRs@PEG_{Low} and AuNRs@PEG_{High}, molecular peak patterns for CTA^{+} ions (**Figures 3B, S3 and S4**) and also for PEG (**Figure S5**) were observed at *m/z* 284 and 4898/4940,respectively. These are the only molecular ions that can be identified in the mass spectra, *m/z* 284 being the most intense peak, which shows the higher ability of CTAB molecules to be ionized. By using LDI-MS, we are able to detect an ion signal (m/z 284) for AuNRs@PEG_{Low} particles that is one order of magnitude higher than that for AuNRs@PEG_{High} (**Figure 3B**), thereby confirming the large difference in the extent of CTAB removal during PEG grafting. We thus propose that LDI-MS is an accurate technique to directly assess the identity of ligands that are present at a very low density. This technique has the added benefit over NMR spectroscopy that a lower sample volume is required. The LDI-MS results support the findings obtained by AGE, zeta potential and LC-MS/MS analysis and strongly suggest that AuNRs@PEG_{High} and AuNRs@PEG_{Low} comprise low and high levels of CTAB respectively.

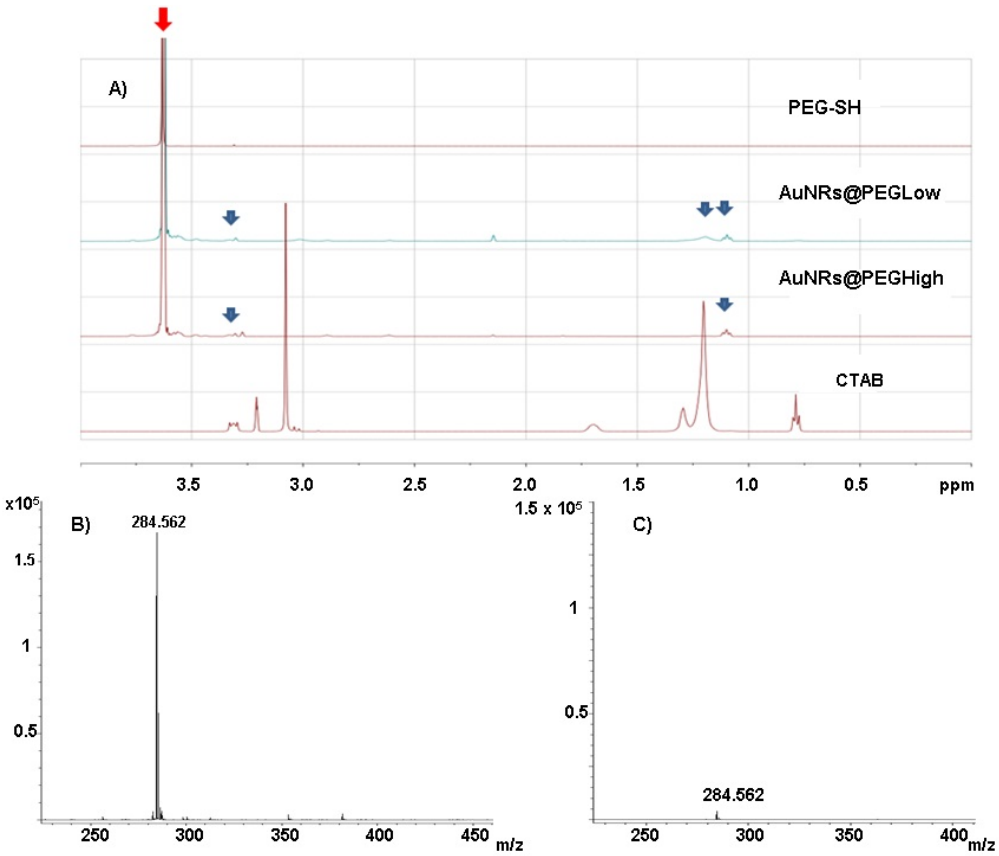

Figure 3. A) ^{1}H NMR spectra of AuNRs@PEG$_{High}$, AuNRs@PEG$_{Low}$ and the corresponding free ligands (PEG-SH and CTAB). Blue arrows indicate typical CTAB signals in AuNR samples and the red arrow pointsatthe intense peak (3.6 ppm singlet) assigned to PEG. B,C) LDI mass spectra of AuNRs@PEG$_{Low}$ (B) and AuNRs@PEG$_{High}$ (C). The m/z ratio at 284 corresponds to CTA^{+} ions.

An important finding from the LDI-MS characterization of AuNRs is that even when a large excess of PEG-SH was used to replace CTAB (AuNRs@PEG$_{High}$), a small fraction of CTAB still remains present on the particles, which may be of relevance regarding cytotoxicity and consequently cellular uptake mechanisms. As it was apparent that complete CTAB removal would be difficult, we investigated the possibility of using residual CTAB as a mass barcode to analyze the uptake efficiency of AuNRs@PEG$_{High}$ by cells. Previous studies showed that a high density of PEG molecules on gold nanoparticles minimizes the adsorption of serum proteins and

in turn their internalization by macrophages,[39,40] which is of interest in practical applications so that in vivo targeting can be achieved.[41] We thus cultured macrophage-like J774 cells together with AuNRs@PEG_{High} (low CTAB levels) at two different concentrations (2.5×10^5 and 6.25×10^4 particles/mL). After 4hand 24h, the supernatants containing non-phagocytized material were removed and the adherent cells lysed for identification of the CTA^+ signal (m/z 284) in the MS spectra. We confirmed that AuNRs@PEG_{High} (2.5×10^5 Au NRs/mL) are non-toxic to J774 cells and even after 24h of incubation no cell morphology changes were observed, with excellent cell survival data for all tested concentrations (**Figure S6**). The relative CTA^+ ion signal intensity of AuNRs@PEG_{High} detected in cell lysates showed a clear dependence on both concentration and time (**Figure 4A**). As expected, high concentrations (2.25×10^5 particles/mL) and longer incubation times (24 hours) resulted in higher levels of AuNR uptake by macrophages. At the shorter time point of 4h we were able to detect the presence of AuNRs@PEG_{High} with a signal to noise ratio of >1000, thus rendering this technique more sensitive than previously described work for imaging of high-density PEGylated AuNPs using dark field microscopy of incubated macrophage cells at short time (4 hours) and similar concentration.[41] A key issue in the use of LDI-MS is that the measurements were carried out without any MALDI matrix, which guarantees that the signal arises exclusively from CTAB molecules attached to gold particles andnot from free ligands. This was confirmed by the absence of CTAB signal in matrix-free LDI-MS analysis of the solution resulting from complete AuNR etching with cyanide (**Figure S7**). The use of LDI-MS to evaluate nanoparticle uptake in cells therefore offers an interesting alternative to the use of fluorescent or radioactively tagged nanoparticles, both of which suffer from complications in the chemical conjugation and ensuring that tags remain with the nanoparticles. Our results additionally indicate that CTAB molecules remain adsorbed to the

AuNRs surface, even after long incubation times, as the CTA^+ signal would not be detected if CTAB were free in solution. For small molecules as CTAB the desorption/ionization mass analysis usually requires using an agent that provides efficient ionization with minimal or controlled fragmentations, e.g. MALDI matrices or other alternative materials. The use of LDI-MS thus provides a highly sensitive and selective assay for AuNR detection by ionizing adsorbed CTAB ligands. In order to determine the limit of detection (LOD) of AuNR@PEG in cells using LDI-MS, we incubated J774 cells with a range of AuNR@PEG concentrations and analyzed both the non-phagocytized (supernatant) and phagocytized (cellular) fractions (**Figure 4B**). As expected, a clear concentration effect was noted in the cellular lysates with an LOD as low as 1.6×10^3 particles/mL being detected. Importantly, no detectable CTA^+ ion signal was obtained from the supernatants, suggesting that the ability of J774 cells to phagocytize AuNR@PEG particles was higher than initially assumed and that the cells phagocytized all of the added NRs.

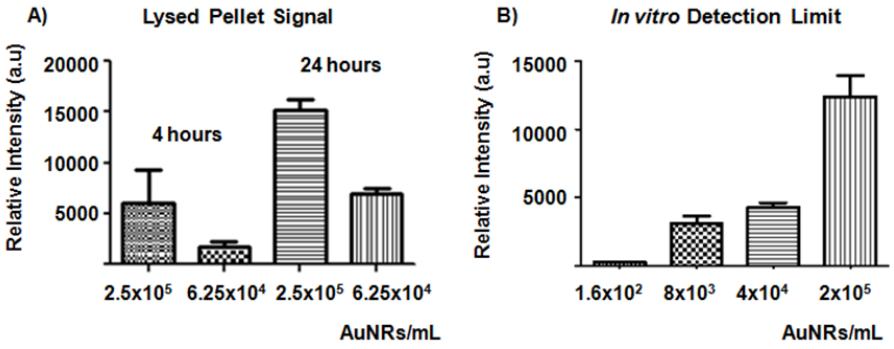

Figure 4.A) Comparison of relative CTA^+ ion signal intensity from AuNRs@PEG_{High} particles after incubation with J774 cells and analyzed by LDI-MS. J774 macrophage cell line was incubated for 4 or 24 hours at 37 ºC with two different concentrations (2.5×10^5 and 6.25×10^4 particles/mL). After removal of the supernatant and extensive washing to remove free particles, the cells were lysed and spotted onto a MALDI plate for LDI-MS analysis. The LDI mass spectra of J774 cell lysates after AuNR uptake show a peak at m/z 284 corresponding to CTA^+. B) CTA^+ ion signal intensities in cell lysates after J774 cells were incubated for 24 hours with

different concentrations of AuNRs@PEG_{High}. The cellular lysates and supernatants were then analyzed by LDI-MS. Whereas supernatants did not show any detectable CTA^+ ion signal, a strong concentration effect was noted for the lysed cell samples.

In summary, we employed LDI-MS analysis to study changes in CTAB content on PEG-ylated AuNRs. CTA^+ ions are profusely generated by LDI when adsorbed on AuNRs (but not when in solution), thereby providing a straightforward means to detect the presence ofAuNRs, even at low concentrations. Agarose gel electrophoresis was additionally used as a reliable and sensitive analytical method to provide information about the influence of changes in ligand grafting density on protein binding. Finally, the selective ionization by LDI–MS of residual CTAB immobilized on gold surfaces was applied to evaluate the uptake of AuNRs@PEG by macrophages. Our study indicates that this technique and specifically the use of the CTAB as a label, has a great potential for probing the *in vitro* interactions of AuNRs with complex fluids and cellular systems.

ASSOCIATED CONTENT

Supporting Information. Experimental details and various figures and tables including additional agarose gels and characterization data. This material is available free of charge via the Internet at http://pubs.acs.org.

AUTHOR INFORMATION

Corresponding Authors

*Email: spenades@cicbiomagune.es; llizmarzan@cicbiomagune.es

Notes

The authors declare no competing financial interests.

ACKNOWLEDGMENT

This work was supported by the Spanish Ministry of Economy and Competitiveness (MAT2013-46101-R) and the Basque Department of Economic Development and Competitiveness (ETORTEK). We thank Dr. Javier Calvo for mass spectrometry support.

REFERENCES

(1) Eustis, S.; El-Sayed, M. A. Why Gold Nanoparticles Are More Precious than Pretty Gold: Noble Metal Surface Plasmon Resonance and Its Enhancement of the Radiative and Nonradiative Properties of Nanocrystals of Different Shapes. *Chem. Soc. Rev.* **2006**, *35*, 209–217.

(2) Huang, X.; El-Sayed, I. H.; El-Sayed, M. A. Applications of Gold Nanorods for Cancer Imaging and Photothermal Therapy. *Methods Mol. Biol.* **2010**, *624*, 343–357.

(3) Yu, C.; Irudayaraj, J. Multiplex Biosensor Using Gold Nanorods. *Anal. Chem.* **2007**, *79*, 572–579.

(4) Pérez-Juste, J.; Pastoriza-Santos, I.; Liz-Marzán, L. M.; Mulvaney, P. Gold Nanorods: Synthesis, Characterization and Applications. *Coord. Chem. Rev.* **2005**, *249*, 1870–1901.

(5) Mayer, K. M.; Lee, S.; Liao, H.; Rostro, B. C.; Fuentes, A.; Scully, P. T.; Nehl, C. L.; Hafner, J. H. A Label-Free Immunoassay Based upon Localized Surface Plasmon Resonance of Gold Nanorods. *ACS Nano* **2008**, *2*, 687–692.

(6) Alkilany, A. M.; Nagaria, P. K.; Hexel, C. R.; Shaw, T. J.; Murphy, C. J.; Wyatt, M. D. Cellular Uptake and Cytotoxicity of Gold Nanorods: Molecular Origin of Cytotoxicity and Surface Effects. *Small* **2009**, *5*, 701–708.

(7) Leonov, A. P.; Zheng, J.; Clogston, J. D.; Stern, S. T.; Patri, A. K.; Wei, A. Detoxification of Gold Nanorods by Treatment with Polystyrenesulfonate. *ACS Nano* **2008**, *2*, 2481–2488.

(8) Hauck, T. S.; Ghazani, A. A.; Chan, W. C. Assessing the Effect of Surface Chemistry on Gold Nanorod Uptake, Toxicity, and Gene Expression in Mammalian Cells. *Small* **2008**, *4*, 153–159.

(9) Takahashi, H.; Niidome, Y.; Niidome, T.; Kaneko, K.; Kawasaki, H.; Yamada, S. Modification of Gold Nanorods Using Phosphatidylcholine to Reduce Cytotoxicity. *Langmuir* **2006**, *22*, 2–5.

(10) Niidome, T.; Yamagata, M.; Okamoto, Y.; Akiyama, Y.; Takahashi, H.; Kawano, T.; Katayama, Y.; Niidome, Y. PEG-Modified Gold Nanorods with a Stealth Character for in Vivo Applications. *J. Control. Release* **2006**, *114*, 343–347.

(11) Karakoti, A. S.; Das, S.; Thevuthasan, S.; Seal, S. PEGylated Inorganic Nanoparticles. *Angew. Chem. Int. Ed.* **2011**, *50*, 1980–1994.

(12) García I, Sánchez-Iglesias A, Henriksen-Lacey M, Grzelczak M, Penadés S, L.-M. L. Glycans as Biofunctional Ligands for Gold Nanorods: Stability and Targeting in Protein-Rich Media. *J. Am. Chem. Soc.* **2015**, *137*, 3686-3692.

(13) Khanal, B. P.; Zubarev, E. R. Rings of Nanorods. *Angew. Chem. Int. Ed.* **2007**, *46*, 2195–2198.

(14) Oyelere, A. K.; Chen, P. C.; Huang, X.; El-Sayed, I. H.; El-Sayed, M. A. Peptide-Conjugated Gold Nanorods for Nuclear Targeting. *Bioconjug. Chem.* **2007**, *18*, 1490–1497.

(15) Basiruddin, S. K.; Saha, A.; Pradhan, N.; Jana, N. R. Functionalized Gold Nanorod Solution via Reverse Micelle Based Polyacrylate Coating. *Langmuir* **2010**, *26*, 7475–7481.

(16) Kinnear, C.; Dietsch, H.; Clift, M. J.; Endes, C.; Rothen-Rutishauser, B.; Petri-Fink, A. Gold Nanorods: Controlling Their Surface Chemistry and Complete Detoxification by a Two-Step Place Exchange. *Angew. Chem. Int. Ed.* **2013**, *52*, 1934–1938.

(17) Albanese, A.; Tang, P. S.; Chan, W. C. The Effect of Nanoparticle Size, Shape, and Surface Chemistry on Biological Systems. *Annu. Rev. Biomed. Eng.* **2012**, *14*, 1–16.

(18) McLean, J. A.; Stumpo, K. A.; Russell, D. H. Size-Selected (2-10 nm) Gold Nanoparticles for Matrix Assisted Laser Desorption Ionization of Peptides. *J. Am. Chem. Soc.* **2005**, *127*, 5304–5305.

(19) Nagahori, N.; Nishimura, S. Direct and Efficient Monitoring of Glycosyltransferase Reactions on Gold Colloidal Nanoparticles by Using Mass Spectrometry. *Chem.Eur. J.* **2006**, *12*, 6478–6485.

(20) Huang, Y. F.; Chang, H. T. Analysis of Adenosine Triphosphate and Glutathione through Gold Nanoparticles Assisted Laser Desorption/ionization Mass Spectrometry. *Anal. Chem.* **2007**, *79*, 4852–4859.

(21) Sudhir, P. R.; Wu, H. F.; Zhou, Z. C. Identification of Peptides Using Gold Nanoparticle-Assisted Single-Drop Microextraction Coupled with AP-MALDI Mass Spectrometry. *Anal. Chem.* **2005**, *77*, 7380–7385.

(22) Castellana, E. T.; Gamez, R. C.; Gomez, M. E.; Russell, D. H. Longitudinal Surface Plasmon Resonance Based Gold Nanorod Biosensors for Mass Spectrometry. *Langmuir* **2010**, *26*, 6066–6070.

(23) Pinaud, F.; King, D.; Moore, H. P.; Weiss, S. Bioactivation and Cell Targeting of Semiconductor CdSe/ZnS Nanocrystals with Phytochelatin-Related Peptides. *J. Am. Chem. Soc.* **2004**, *126*, 6115–6123.

(24) Howarth, M.; Liu, W.; Puthenveetil, S.; Zheng, Y.; Marshall, L. F.; Schmidt, M. M.; Wittrup, K. D.; Bawendi, M. G.; Ting, A. Y. Monovalent, Reduced-Size Quantum Dots for Imaging Receptors on Living Cells. *Nat. Methods* **2008**, *5*, 397–399.

(25) Salvati, A.; Pitek, A. S.; Monopoli, M. P.; Prapainop, K.; Bombelli, F. B.; Hristov, D. R.; Kelly, P. M.; Aberg, C.; Mahon, E.; Dawson, K. A. Transferrin-Functionalized Nanoparticles Lose Their Targeting Capabilities When a Biomolecule Corona Adsorbs on the Surface. *Nat. Nanotechnol.* **2013**, *8*, 137–143.

(26) Monopoli, M. P.; Aberg, C.; Salvati, A.; Dawson, K. A. Biomolecular Coronas Provide the Biological Identity of Nanosized Materials. *Nat. Nanotechnol.* **2012**, *7*, 779–786.

(27) Lou, X.; van Dongen, J. L.; Vekemans, J. A.; Meijer, E. W. Matrix Suppression and Analyte Suppression Effects of Quaternary Ammonium Salts in Matrix-Assisted Laser Desorption/ionization Time-of-Flight Mass Spectrometry: An Investigation of Suppression Mechanism. *Rapid. Commun. Mass. Spectrom.* **2009**, *23*, 3077–3082.

(28) Chithrani, B. D.; Chan, W. C. Elucidating the Mechanism of Cellular Uptake and Removal of Protein-Coated Gold Nanoparticles of Different Sizes and Shapes. *Nano Lett.* **2007**, *7*, 1542–1550.

(29) Curry, A. C.; Crow, M.; Wax, A. Molecular Imaging of Epidermal Growth Factor Receptor in Live Cells with Refractive Index Sensitivity Using Dark-Field Microspectroscopy and Immunotargeted Nanoparticles. *J. Biomed. Opt.* **2008**, *13*, 14022.

(30) Zavaleta, C. L.; Smith, B. R.; Walton, I.; Doering, W.; Davis, G.; Shojaei, B.; Natan, M. J.; Gambhir, S. S. Multiplexed Imaging of Surface Enhanced Raman Scattering Nanotags in Living Mice Using Noninvasive Raman Spectroscopy. *Proc. Natl. Acad. Sci. U. S. A.* **2009**, *106*, 13511–13516.

(31) Zhu, Z.-J.; Yeh, Y.-C.; Tang, R.; Yan, B.; Tamayo, J.; Vachet, R. W.; Rotello, V. M. Stability of Quantum Dots in Live Cells. *Nat. Chem.* **2011**, *3*, 963–968.

(32) Zhu, Z. J.; Ghosh, P. S.; Miranda, O. R.; Vachet, R. W.; Rotello, V. M. Multiplexed Screening of Cellular Uptake of Gold Nanoparticles Using Laser Desorption/ionization Mass Spectrometry. *J. Am. Chem. Soc.* **2008**, *130*, 14139–14143.

(33) Levy, R.; Shaheen, U.; Cesbron, Y.; See, V. Gold Nanoparticles Delivery in Mammalian Live Cells: A Critical Review. *Nano Rev.* **2010**, *1*, 4889. DOI: 10.3402/nano.v1i0.4889.

(34) Mout, R.; Moyano, D. F.; Rana, S.; Rotello, V. M. Surface Functionalization of Nanoparticles for Nanomedicine. *Chem. Soc. Rev.* **2012**, *41*, 2539–2544.

(35) Perry, J. L.; Reuter, K. G.; Kai, M. P.; Herlihy, K. P.; Jones, S. W.; Luft, J. C.; Napier, M.; Bear, J. E.; DeSimone, J. M. PEGylated PRINT Nanoparticles: The Impact of PEG Density on Protein Binding, Macrophage Association, Biodistribution, and Pharmacokinetics. *Nano Lett.* **2012**, *12*, 5304–5310.

(36) Cifuentes-Rius, A.; de Puig, H.; Kah, J. C.; Borros, S.; Hamad-Schifferli, K. Optimizing the Properties of the Protein Corona Surrounding Nanoparticles for Tuning Payload Release. *ACS Nano* **2013**, *7*, 10066–10074.

(37) Rezwan, K.; Meier, L. P.; Gauckler, L. J. Lysozyme and Bovine Serum Albumin Adsorption on Uncoated Silica and AlOOH-Coated Silica Particles: The Influence of Positively and Negatively Charged Oxide Surface Coatings. *Biomaterials* **2005**, *26*, 4351–4357.

(38) Fischer, H. C.; Hauck, T. S.; Gomez-Aristizabal, A.; Chan, W. C. Exploring Primary Liver Macrophages for Studying Quantum Dot Interactions with Biological Systems. *Adv. Mater.* **2010**, *22*, 2520–2524.

(39) Walkey, C. D.; Olsen, J. B.; Guo, H.; Emili, A.; Chan, W. C. Nanoparticle Size and Surface Chemistry Determine Serum Protein Adsorption and Macrophage Uptake. *J. Am. Chem. Soc.* **2012**, *134*, 2139–2147.

(40) Larson, T. A.; Joshi, P. P.; Sokolov, K. Preventing Protein Adsorption and Macrophage Uptake of Gold Nanoparticles via a Hydrophobic Shield. *ACS Nano* **2012**, *6*, 9182–9190.

(41) Moghimi, S. M.; Hunter, A. C.; Murray, J. C. Long-Circulating and Target-Specific Nanoparticles: Theory to Practice. *Pharmacol. Rev.* **2001**, *5*, 283–318.